Heterogeneous Cobalt-Catalyzed H_2S-Reagent-Free Dialkylpolysulfane Synthesis from Alkenes, Elemental Sulfur, and Hydrogen

Yamamoto, Eiji
Department of Chemistry, Graduate School of Science, Kyushu University

Takaki, Yuta
Department of Chemistry, Graduate School of Science, Kyushu University

Kawai, Yasutaka
Department of Chemistry, Graduate School of Science, Kyushu University

Takakura, Kei
Department of Chemistry, Graduate School of Science, Kyushu University

他

出版情報：ACS Catalysis. 13 (21), pp.14121-14130, 2023-10-19. American Chemical Society (ACS)
バージョン：

Heterogeneous Cobalt-Catalyzed H_2S-Reagent-Free Dialkylpolysulfane Synthesis from Alkenes, Elemental Sulfur, and Hydrogen

Eiji Yamamoto,[a] Yuta Takaki,[a] Yasutaka Kawai,[a] Kei Takakura,[a] Moemi Kimura,[a] Haruno Murayama,[a] Takafumi Nagao,[b] Takashi Kamachi,*[b] Hironobu Matsueda,[c] Shujiro Otsuki,[c] Hiroshi Sakata,[c] and Makoto Tokunaga*[a]*

[a]Department of Chemistry, Graduate School of Science, Kyushu University, 744 Motooka, Nishi-ku, Fukuoka, 819-0395, Japan

[b]Department of Life, Environment and Applied Chemistry, Fukuoka Institute of Technology, 3-30-1 Wajiro-higashi, Higashi-ku, Fukuoka, 811-0295, Japan

[c]Processing Technical Group 3, DIC Corporation, Ibaraki 314-0193, Japan

KEYWORDS: cobalt, dialkylpolysulfanes, heterogeneous catalyst, heterolytic H_2 activation, hydrogen

ABSTRACT Herein, we report a novel heterogeneous cobalt-catalyzed H_2S-reagent-free synthetic method for 1,2-bis(2,4,4-trimethylpentan-2-yl)polysulfanes, which have been used as extreme-pressure additives in the field of tribology, and have been produced worldwide in the tens of thousands of tonnes per year. The current industrial synthetic processes typically use hydrogen

sulfide as the reductant, but improvements are needed in terms of the toxicity and the cost associated with safety control. The present reaction with Co_3O_4 and Na-X zeolite as catalysts provides the corresponding polysulfanes with three to eight sulfur atoms from diisobutylene, hydrogen, and elemental sulfur in up to 88% yield under neat reaction conditions. Experimental and density functional theory (DFT) mechanistic investigations provide insights into the roles of Na-X zeolite and cobalt catalysts. The DFT calculations suggest heterolytic H_2 activation with cobalt polysulfide species and subsequent protonation of alkenes and the C–S bond formation take place in a single step by a terminal SSH group in the cobalt polysulfide species, which provides a reasonable interpretation of the observed Markovnikov selectivity.

Dialkylpolysulfanes (RS_nR, $n \geq 2$), which contain chains of sulfur atoms, are important organosulfur chemicals, have a wide range of applications in a variety of fields such as life and material science.[1] In the field of tribology, dialkylpolysulfanes have often been employed as extreme-pressure (EP) additives, which are essential ingredients for most industrial lubricants that protect equipment from wear and seizure.[2] For this purpose, dialkylpolysulfanes have been produced worldwide in the tens of thousands of tonnes per year.

1,2-Bis(2,4,4-trimethylpentan-2-yl)polysulfanes that contain two to eight sulfur atom chains (**2a′–8a′**) derived from diisobutylene (DIB) is one of the above-mentioned high-value organosulfur compounds that has been extensively used as high-viscosity EP additives in the form of a mixture with different sulfur chain lengths (Scheme 1).[3] The present industrial synthetic processes for the compounds have suffered from using hydrogen sulfide. Over the past few decades, various synthetic methods for dialkylpolysulfanes have been developed. For example, Vineyard developed

a base-catalyzed synthetic method of polysulfanes from thiols and elemental sulfur.[4] Yamaguchi and co-workers reported a Rh-catalyzed S–S bond-exchange reaction of dialkyldisulfanes and elemental sulfur.[5] In 2021, the Hilt group reported electrochemical synthetic methods from dialkyldisulfanes and elemental sulfur (Scheme 1a).[6] These reactions can provide polysulfanes under mild reaction conditions. However, the starting organosulfur substrates need to be prepared from feedstock materials using sulfurizing agents, which results in increasing the synthetic cost. With reference to the industrial processes, a radical-mediated synthetic method from alkenes and elemental sulfur, called black sulfurization, is the simplest and oldest one,[2] providing the most economical route to obtain dialkylpolysulfanes (Scheme 1b). However, the polysulfane products manufactured via black sulfurization contain various organosulfur derivatives such as thioketones, thiophenes, and other unsaturated sulfur compounds, which cause the products to be dark and smelly, and make them lack long-term stability due to the remaining reactive unsaturated sulfur compounds, which limits the use of the polysulfane products. Among the more sophisticated methods, catalytic synthetic processes that directly provide dialkylpolysulfanes from diisobutylene, elemental sulfur, and hydrogen sulfide is a potent synthetic method providing the polysulfane products without conjugated impurities, and employed as a recent industrial process (Scheme 1c).[1b,7] However, the use of H_2S has drawbacks such as its toxicity, corrosiveness, and unpleasant odor, making it difficult to handle and increasing the costs associated with the equipment and management. Thus, the use of an alternative safer and cheaper reductant for H_2S is highly desirable.

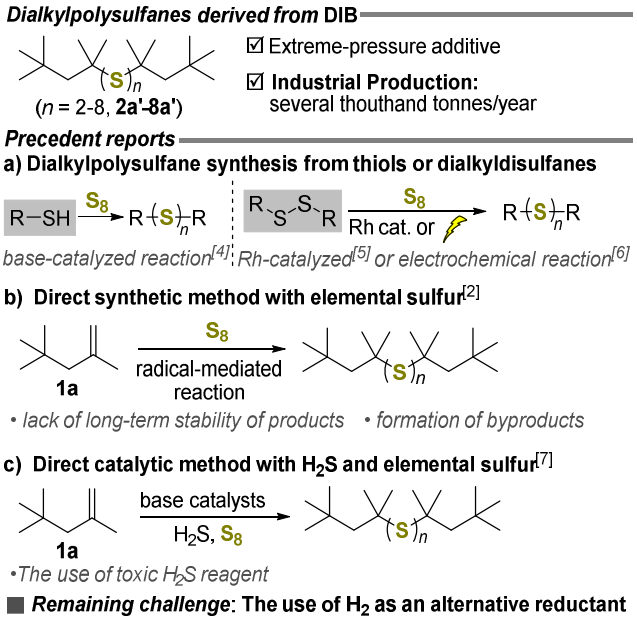

Scheme 1. Synthetic methods of dialkylpolysulfanes.

In this context, hydrogen is one of the potent alternative reductants; however, a synthetic method for polysulfanes using hydrogen has not hitherto been reported. In the field of organic synthesis, elemental sulfur has been employed as an important sulfurizing reagent and has been used in combination with various reducing agents such as hydrosilanes and metal hydrides.[8] However, examples of elemental sulfur in combination with molecular hydrogen are extremely limited, probably due to the difficulty in activating hydrogen under sulfur-rich reaction conditions. Thus, developing a H_2S-free polysulfane synthesis from olefins, elemental sulfur, and hydrogen is an important and challenging issue. Our group has been working on developing effective synthetic transformations with heterogeneous catalysts.[9] We envisioned that the use of Co catalysts, used in the thiol synthesis from carbonyl compounds with elemental sulfur and molecular hydrogen,[10] would potentially promote hydrogenolysis of the S–S bond of elemental sulfur to form dihydropolysulfanes (HS_nH), followed by subsequent addition of a sulfhydryl group and S–S bond-exchange reactions to produce the desired dialkylpolysulfanes.

Herein, we report the first H_2S-reagent-free dialkylpolysulfane synthesis from olefins, elemental sulfur, and hydrogen using Co_3O_4 as a precatalyst under neat reaction conditions (Scheme 2, This Work). This catalytic system provided the desired 1,2-bis(2,4,4-trimethylpentan-2-yl)polysulfanes in up to 88% yield, which is comparable to the current industrial process. In addition, the catalyst exhibited excellent reusability. Significant yield loss was not observed after at least 10 reuses. Furthermore, a 10-g scale reaction was also successful. Experimental and density functional theory (DFT) mechanistic studies were also conducted. In addition, characterization of the Co catalysts before and after the reaction was conducted using powder X-ray diffraction (XRD), X-ray photoelectron spectroscopy (XPS), high-angle annular dark-field scanning transmission electron microscopy (HAADF–STEM), and energy dispersive X-ray spectroscopy (EDS) analyses. The results suggested that Co_3O_4 was subjected to sulfurization under the reaction conditions. As for the reaction mechanism, a control reaction in the presence of a radical scavenger indicated that radical mechanisms were not involved. DFT calculations with CoS_2 as a model catalyst indicated a heterolytic H_2 activation with cobalt polysulfide species and subsequent protonation and Markovnikov-type C–S bond formation in a single step with a terminal SSH group in the cobalt polysulfide species. Na-X zeolite additive, as a solid base, improved the yield under low-hydrogen-pressure reaction conditions.

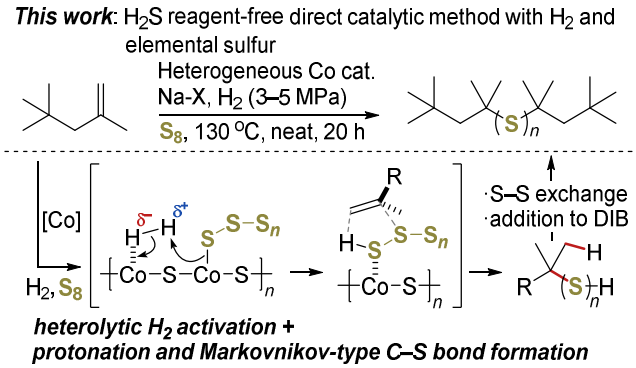

Scheme 2. Heterogeneous Co-catalyzed polysulfane synthesis from alkenes, elemental sulfur, and hydrogen.

2. Experimental Section

2.1. Chemical and Catalyst Materials.

Unless otherwise stated, all the commercially available reagents were used without purification. Co_3O_4 (nanopowder, <50 nm particle size (TEM), 99.5% trace metals basis), sulfur powder, Molecular Sieves 13X (Na-X, powder, < 2μm average particle size), Molecular Sieves 4A (Na-A, powder, activated, <325 mesh particle size) and 2,4,4-trimethyl-2-pentene were purchased from Sigma-Aldrich. $Co(OAc)_2$, $Co(NO_3)_2 \cdot 6H_2O$, Na_2CO_3, dicyclohexylamine and NaOH were purchased from FUJIFILM Wako Pure Chemical Corporation. 2-propanol (LC/MS grade), acetonitrile (LC/MS grade) and distilled water (LC/MS grade) were purchased from Kanto Chemical Co., Inc. CoS was purchased from Strem Chemicals, Inc. Molecular Sieves 3A (K-A) was purchased from GL Sciences Inc. 2,4,4-trimethyl-1-pentene, bis(2,4-pentanedionato)cobalt(II) and tris(2,4-pentanedionato)cobalt(III) were purchased from Tokyo Chemical Industry Co., Ltd. CoS_2 (powder, <200 mesh particle size, 99.5% (metals basis excluding

Ni, Ni <0.2%)) was purchased from Alfa Aesar. Authentic sample of disulfane **2'a** was purchased from Tokyo Chemical Industry Co., Ltd. Dialkyltrisulfane **3'a** was provided from DIC Corporation. Dialkyltetrasulfane **4'a** was prepared according to the literature.[1a] Dialkylpentasulfane **5'a** and dialkylhexasulfane **6'a** were synthesized by the reaction of polysulfane synthesis in this manuscript, and purified by preparative HPLC using a JASCO PU-1580 (detector: UV/VIS) equipped with InertSustain C8 column (5 μm, 10 mm x 250 mm). The conditions for preparative HPLC are as follows. Mobile phase: 2-propanol/MeCN/H_2O = 2/2/1, Flow rate: 4 mL/min, Wavelength: 210 nm. High-resolution mass (HRMS) analyses were measured on JEOL JMS-700 mass spectrometer at Evaluation Center of Materials Properties and Function, Institute for Materials Chemistry and Engineering, Kyushu University.

2.2. Catalyst Characterization.

2.2.1. Measurement of Specific Surface Area. Nitrogen adsorption isotherms were measured at −196 °C using a BELSORP-mini II. The samples were degassed for 120 min at 100 °C before measurement. The specific surface areas of the samples were calculated according to the multipoint Brunauer-Emmett-Teller (BET) procedure.

2.2.2. Measurement of Cobalt elution. Aqua regia was added to the polysulfane products (scheme 3) and heated at 260°C until it became a transparent aqueous solution. After that, the amount of cobalt eluted in the products was calculated from the concentration of aqueous solution measured by Agilent 4100 MP-AES (Agilent Technologies).

2.2.2. X-Ray Structure Analyses. Powder X-ray diffraction (XRD) patterns were obtained on a Rigaku MiniFlex600 with a high-intensity Cu K_α radiation source (λ = 0.15418 nm). XPS spectra were recorded on AXIS ULTRA DLD spectrometer (SHIMADZU CORPORATION) equipped

with an Al Kα radiation source at a pressure below 10^{-7} Pa. The charge neutralizer system was used. Photoelectron peak C 1s (284.8 eV) was used for a binding energy correction. The collected spectra were analyzed by using XPSPEAK 4.1 after applying a Shirley background subtraction and Gaussian decomposition parameters. STEM and EDS were performed using a JEOL JEM-ARM200F microscope operated at 200 kV.

2.3. General Procedures.

2.3.1. General Procedures for Polysulfane Synthesis. Sulfur powder (1.92 g, 60 mmol as a sulfur atom), Co_3O_4 (80.3 mg, Co: 1 mmol), Na-X [100 mg including moisture (24 wt% of H_2O)], 2,4,4-trimethylpentene (20 mmol) and a stirring bar were placed in a 40 mL autoclave. The autoclave was evacuated and charged with H_2 gas three times. Then, the autoclave was heated and stirred at 800 rpm. After the reaction, the autoclave was cooled to 0 ºC, and then 1,3,5-tri-*tert*-butylbenzene (200 mg) was added as an internal standard. The resulting mixture was then centrifuged and filtered to remove the catalyst. The resultant solution was analyzed using ^{1}H NMR and UPLC. Yields of dialkylpolysulfanes [**2'a**–**6'a** (*n* = 2–6)] were obtained by Ultra Performance Liquid Chromatography (UPLC) analysis using a waters ACQUITY UPLC H-Class system equipped with PDA (total absorbance 210–800 nm) and a Kinetex-C8 column (2.6 μm, 2.1 mm x 150 mm) with the prepared authentic samples. The yields of the dialkylpolysulfanes **7'a** (*n* = 7) and **8'a** (*n* = 8) were estimated from the UPLC peak areas using coefficients obtained by extrapolating from the correlation between the absorbance of the dialkylpolysulfanes and the number of S–S bonds (See, Figure S1 in Supporting Information). The conditions for UPLC analysis are as follows. Mobile phase: 2-propanol/MeCN/H_2O = 2/1/1, Flow rate: 0.5 mL/min, Wavelength: 210–800 nm.

2.3.2. General procedures for catalyst recycling experiments. Sulfur powder (1.92 g, 60 mmol as a sulfur atom), Co_3O_4 (80.3 mg, 1 mmol/Co), Na-X [100 mg including moisture (24 wt% of H_2O)], 2,4,4-trimethylpentene (20 mmol) and a stirring bar were placed in a 40 mL autoclave. The autoclave was evacuated and charged with H_2 gas for three times. Then, the autoclave was heated and stirred at 800 rpm. After the reaction, the autoclave was cooled at 0 ºC, and then 1,3,5-tri-*tert*-butylbenzene (200 mg) was added as an internal standard. The resulting mixture was centrifuged and filtrated to remove the catalyst. The recovered catalyst was washed with CS_2 (2 mL x 3). After that, the catalyst was dried under reduced pressure, then it was reused in the next experiment.

3. Results and Discussions.

Cobalt-based materials have been used as catalysts for hydrodesulfurization of crude feedstocks in petroleum refineries.[11] Thus, we selected cobalt compounds as catalysts for the polysulfane synthesis from diisobutylene, elemental sulfur, and hydrogen (Figure 1). Co_3O_4, which contains Co(II) and Co(III) species, promoted the reaction to give the corresponding polysulfanes containing three to seven sulfur atom chains in 53% yield, whereas CoO gave a slightly lower polysulfane yield. No anti-Markovnikov-type products were observed. In addition, the reaction in the absence of cobalt catalysts slightly proceeded to give the corresponding polysulfanes in low yield. Furthermore, cobalt(II) complexes such as $Co(OAc)_2$, $Co(acac)_2$, and $Co(NO_3)_2$ as well as $Co(acac)_3$ also showed similar catalytic activity. The cobalt oxides and complexes would be potentially converted to the corresponding cobalt sulfides under the reaction conditions. Thus, we also examined cobalt sulfides such as CoS_2 and CoS. CoS_2 provided the polysulfanes in moderate yields whereas CoS did not promote the reaction, which would be attributable to the low specific surface area of CoS [5.8 m^2/g (CoS_2) vs <0.05 m^2/g (CoS)].

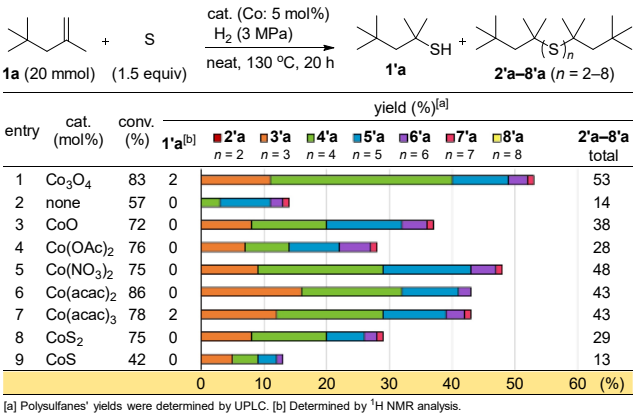

Figure 1. Screening of cobalt catalysts for polysulfane synthesis.

With the Co_3O_4 catalyst in hand, we further optimized the reaction conditions (Figure 2). The use of 3 equiv of elemental sulfur increased the polysulfanes' yield (entry 2, 66%). In addition, we next examined the addition of basic Na-X zeolite, which can promote the thiol–disulfane exchange reaction.[9c] The reaction with Na-X also improved the yield (entry 3, 80%). Furthermore, higher H_2 pressure led to an 88% yield of desired polysulfanes (entry 4) whereas the polysulfanes' yields decreased when the the reaction temperature was varied from 130 °C (entries 5 and 6). The results of the ultra-performance liquid chromatography (UPLC) analysis of the reaction mixture obtained under optimized conditions are presented in Figure 3. In the reaction mixture, dialkyltetrasulfane **4′a** is the main product accounting for about 40% of the polysulfane products. The trisulfane and pentasulfane are each approximately 20%. Other polysulfanes having long sulfur chains with more than six sulfur atoms were also observed but in low yields.

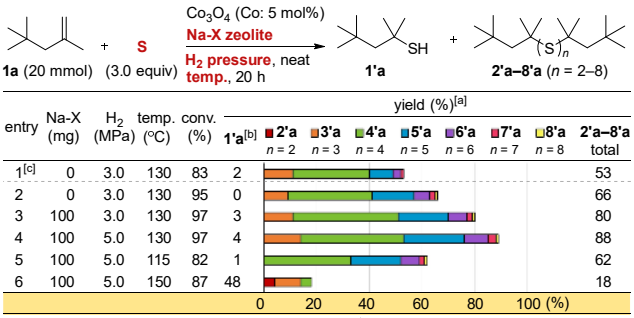

entry	Na-X (mg)	H_2 (MPa)	temp. (°C)	conv. (%)	yield (%)[a] 1'a[b]	2'a n = 2	3'a n = 3	4'a n = 4	5'a n = 5	6'a n = 6	7'a n = 7	8'a n = 8	2'a–8'a total
1[c]	0	3.0	130	83	2								53
2	0	3.0	130	95	0								66
3	100	3.0	130	97	3								80
4	100	5.0	130	97	4								88
5	100	5.0	115	82	1								62
6	100	5.0	150	87	48								18

0 20 40 60 80 100 (%)

[a] Polysulfanes' yields were determined by UPLC. [b] Determined by ^{1}H NMR analysis. [c] The same data is shown in Figure 1, entry1. 1.5 eq of S was used.

Figure 2. Optimization of reaction conditions.

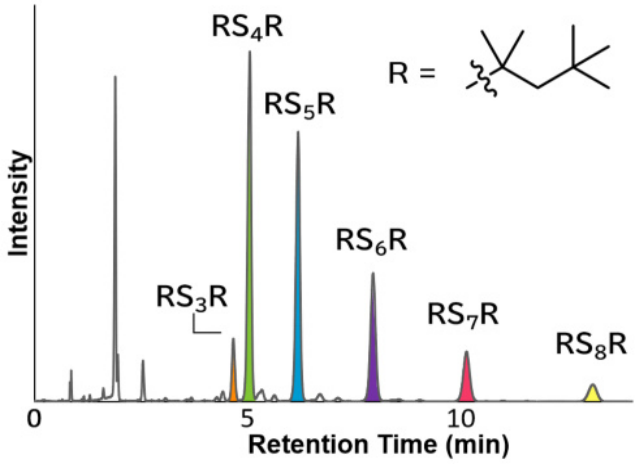

Figure 3. UPLC analysis of the polysulfane products (Figure 2, entry 4). Column: kinetex-C8, Eluent: 2-PrOH/MeCN/H_2O = 2/1/1, Flow Rate: 0.5 mL/min.

To underscore the practicality of the reaction, we then conducted the reaction on a 10-gram scale and performed a catalyst recycling test as well as the reaction with DIB isomer **1b**. The reaction under hydrogen pressure (3 MPa) also proceeded smoothly to provide the corresponding polysulfanes in high total yields as a yellow oil (Scheme 3). In addition, we carried out recycling experiments (Figure 4). The Co_3O_4 and Na-X catalysts were successfully recycled at least 10 times without significant loss of the total polysulfane yields. The reactivity of DIB isomer **1b** is important from the perspective of industrial applications because **1a** and **1b** have been produced

as a mixture from isobutene. The reaction of isomer **1b** under standard reaction conditions also promoted the polysulfane synthesis providing the corresponding desired products in 80% yield with a product distribution similar to that of the reaction mixture obtained under optimized reaction conditions (Scheme 4, for details of the product distributions, see Supplementary Information). It is noteworthy that this result also indicates the applicability to the sterically hindered multi-substituted alkene substrates.

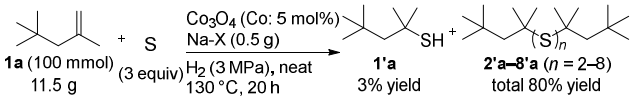

Scheme 3. 10-Gram scale reaction and evaluation for EP additives.

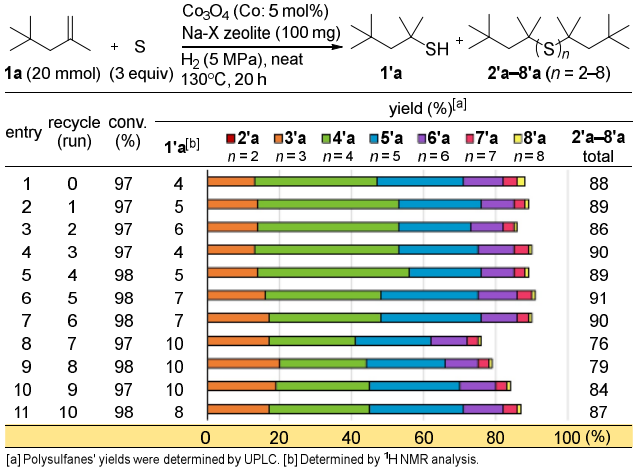

Figure 4. Recycling test of the Co_3O_4 and Na-X catalysts.

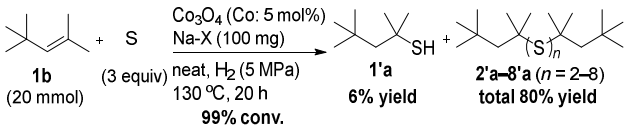

Scheme 4. Polysulfane synthesis from DIB isomer **1b**.

Characterization of the recovered catalyst was performed to obtain insights into the catalyst structure in the reaction. Furthermore, to facilitate the interpretation of the results, a recovered catalyst sample of Co_3O_4 used in the absence of Na-X under the optimized reaction conditions (Figure 2, entry 5) was employed for measurement of specific surface area, XRD, XPS, HAADF–STEM, and EDS analyses. XRD analysis of the recovered Co catalyst showed that the peaks derived from Co_3O_4 (ICSD 36256)[12] fully disappeared, and broad peaks assignable to CoS (ICSD 624857)[13] were observed (Figure 5). These results suggest that Co_3O_4 was subjected to sulfurization to form cobalt sulfide species.[14] Furthermore, considering that CoS has almost no catalytic activity as we presented in Figure 1, the amorphous cobalt sulfide species would serve as the major active species. The Co_3O_4 and the recovered cobalt catalysts were analyzed using the BET method to confirm their specific surface areas. The results showed that the recovered catalyst had a larger specific surface area than the fresh Co_3O_4 (116 m^2/g vs 45 m^2/g). These observations would be attributable to the formation of amorphous cobalt sulfides under the reaction conditions. HAADF–STEM images of the Co catalysts are shown in Figure 6. Granular crystals were observed in the fresh Co_3O_4 catalyst, whereas agglomerated ring structures were observed in the recovered Co catalyst (Figure 6a and 6e). In addition, STEM–EDS spectra showed the presence of Co and S in the recovered Co catalyst, and these elements were also uniformly dispersed over the recovered

Co catalyst. These observations are in good agreement with the results of the XRD analysis, which supports the hypothesis that sulfurization of Co_3O_4 occurred under the reaction conditions.

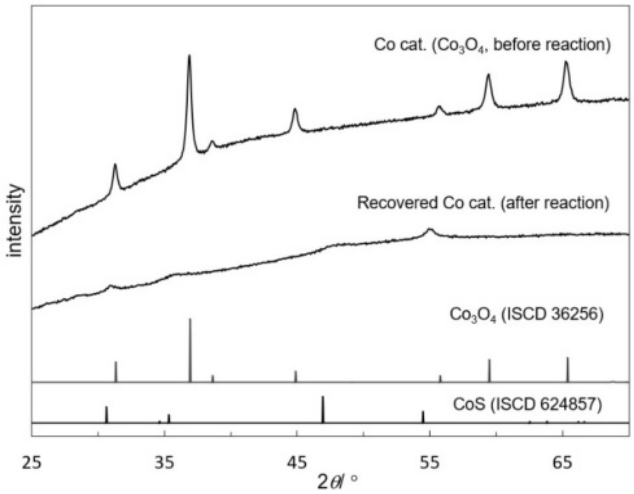

Figure 5. XRD patterns of the recovered Co catalyst and relevant authentic samples.

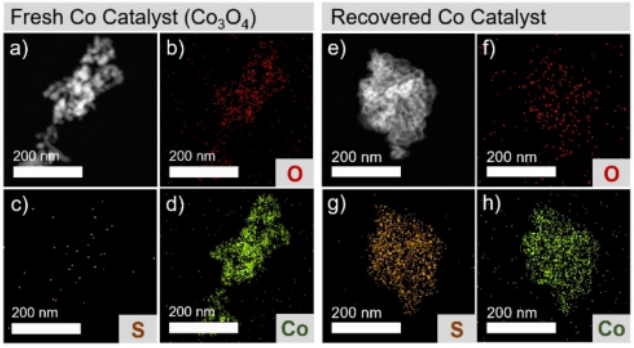

Figure 6. HAADF–STEM images and EDS analysis of the Co catalysts before and after reaction. a) HAADF–STEM image of Co_3O_4, and elemental mapping images of b) O, c) S, d) Co; e) HAADF–STEM image of the recovered Co catalyst and elemental mapping images of f) O, g) S, h) Co.

Next, XPS analysis was performed to investigate the elemental composition and electronic structure of the surface of the recovered Co catalyst (Figure 7). The Co 2p spectrum for the recovered catalyst was deconvoluted into two spin–orbit doublets. The first doublet at 778.8 eV, 793.9 eV and the second at 780.4 eV, 795.5 eV were assigned to Co(III) and Co(II) species, respectively.[15] The relative area ratio of the $2p_{3/2}$ line suggests the Co(III) species was the majority (area ratio of Co(III)/Co(II) = 8.4). Broad satellite peaks were observed at approximately 781.6 eV and 800.4 eV. The S 2p peaks appearing at 162.4 eV and 169.2 eV suggest the existence of S atoms on the recovered catalyst. The peak at 162.4 eV is assignable to the corresponding cobalt sulfides, and a small and broad peak at 169.2 eV is a characteristic of oxidized sulfur atoms.[15]

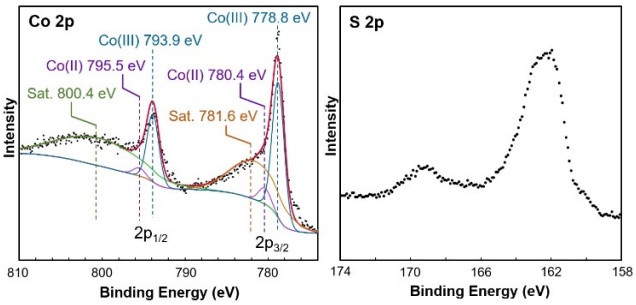

Figure 7. Co 2p and S 2p XPS spectra of the recovered Co catalyst.

To investigate the roles of Na-X, the time course of the reaction and the product distribution were investigated (Figure 8). After 2 h of reaction under 3 MPa hydrogen pressure, the reaction with Na-X showed higher conversion and polysulfane yield than the reaction without Na-X. This result suggests that the addition of Na-X is effective in promoting the reaction as a base catalyst in the nucleophilic addition of a sulfhydryl group. The difference in the conversion and polysulfane yield decreased with time up to 12 h. However, the polysulfane yield after 20 h was about 10%

higher in the reaction with Na-X than in the reaction without Na-X. In contrast to these results, no significant differences in the conversions and yields were observed with or without Na-X in the reaction under 5 MPa H_2 pressure (Figure 8b). Considering these observations, under low H_2 pressure, the S–S bonds of polysulfanes seem less susceptible to hydrogenolysis, which leads to an increase in the polysulfanes with a long sulfur atom chain (n > 8) which do not contribute to the observed polysulfane yield. The increase in the polysulfane yield of the reaction with Na-X under 3 MPa H_2 pressure may be attributable to the acceleration of the S–S bond-exchange reaction between the thiol and polysulfanes with a long sulfur atom chain (n > 8).[9c] Taking these results into consideration, the Na-X catalyst seems to serve as a base catalyst. To assess this hypothesis, we performed the reactions in the presence of various basic additives instead of Na-X under the optimized reaction conditions (see Supporting Information for details). As we expected, the examined basic additives also improved the polysulfane yields, which supports the hypothesis.

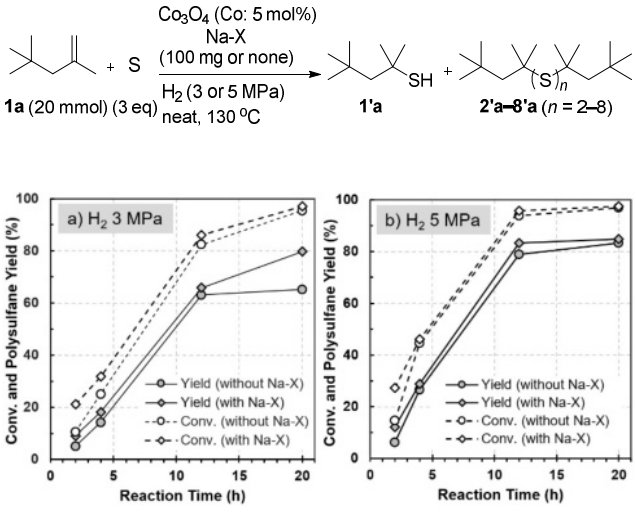

Figure 8. Time course of the Co-catalyzed polysulfane synthesis: a) 3 MPa reaction conditions, b) 5 MPa reaction conditions.

We further performed a control experiment to probe the radical-mediated mechanisms (Scheme 5). The reaction in the presence of 2,6-*t*-butyl-*p*-cresol as a radical scavenger also proceeded to provide the corresponding thiol and polysulfanes in good yield. These results suggest that radical mechanisms are not involved in the catalytic system. In addition, the reaction mixture of this reaction was obtained as yellow oil, which also supports that no radical mechanism was involved in the reaction.

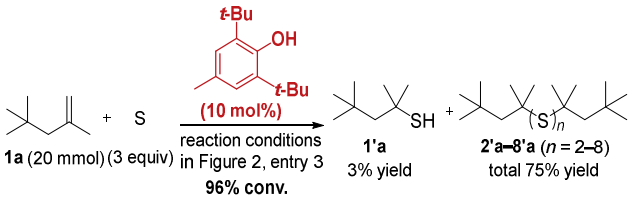

Scheme 5. Control experiment in the presence of a radical scavenger.

As discussed above, catalytic activity is observed for several Co-containing catalysts; however, it is found that they are eventually converted to cobalt sulfide compounds during the catalytic cycle and that CoS_2 shows relatively high activity. The (100) surface is known to be the most stable surface of CoS_2, and previous DFT calculations have intensively examined oxygen reduction reactions on this surface.[16] Although the structure of the active site where the reaction occurs remains unknown, we here used the main surface of CoS_2 as a surface model for DFT calculations to evaluate the fundamental reactivity of the cobalt sulfide species and to gain a better understanding of the reaction mechanism.

First, we examined the most stable adsorption structure of S_8 on clean and sulfur-defective surfaces and the cleavage of the S–S bond of S_8. The adsorption energy of S_8 is −1.80 eV on the clean surface (Figure 9) and −2.24 eV on the sulfur-defective surface (Figure 10), indicating that S_8 adsorbs more strongly on sulfur-defective surfaces due to the stronger binding of S_8 sulfur to Co atoms that become coordinatively unsaturated with the formation of the sulfur defect. As shown in Figure 9, the S_8 molecule adsorbed on the clean surface can undergo S–S bond cleavage with a low activation energy of 0.21 eV. This reaction is almost thermoneutral, and it is likely to easily reach an equilibrium state in which both the S_8 and the intermediate co-exist. The S–S bond can efficiently cleave as well on the sulfur-defective surfaces, stabilizing the system by 0.78 eV; the activation barrier is so low that it is not practical to determine the transition state structure exactly. Interestingly, the resultant intermediate (Int) can undergo further S–S bond cleavage via the transition state shown in Figure 10, resulting in the formation of a linear S_7 molecule adsorbed on the clean surface. The activation barrier for this process is only 0.12 eV, and this step is exothermic by 0.95 eV. Because S_8 is continuously supplied under experimental conditions, any sulfur defects

that can be generated are expected to disappear immediately. Therefore, we focus solely on the clean surface in the following discussion.

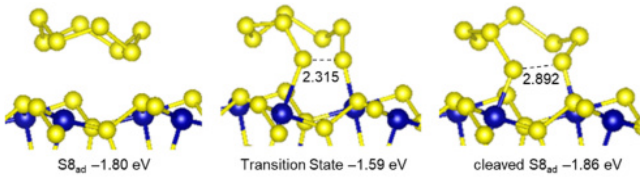

Figure 9. Cleavage of the S–S bond of the S_8 molecule adsorbed on the clean (100) surface of CoS_2. Yellow and blue balls indicate S and Co, respectively. Energies were measured from the total energy of the separated S_8 molecule and surface. Unit is Å.

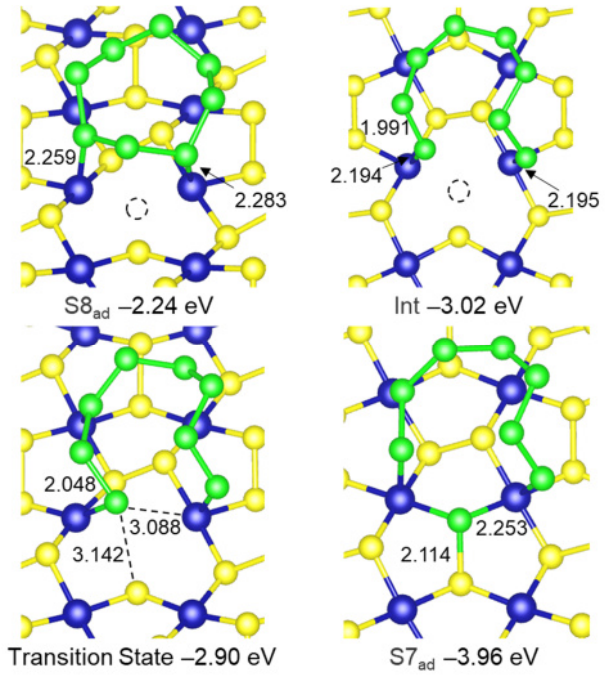

Figure 10. Cleavage of the S–S bond of the S_8 molecule adsorbed on the sulfur-defective (100) surfaces of CoS_2. Energies were measured from the total energy of the separated S_8 molecule and surface. The S_8 molecule is colored green for clarity and the S vacancy site is depicted by dashed circles. Unit is Å.

S–S bonds are usually cleaved homolytically, leading to the formation of S radicals and yielding anti-Markovnikov products when reacting with alkenes. However, Markovnikov-type thiols and polysulfanes are selectively synthesized, suggesting that S radicals are not involved in the reaction. To confirm this, we examined the changes in spin density associated with S–S cleavage. Many Co_xS_y compounds exhibit a metallic and ferromagnetic state, and our DFT calculations showed that CoS_2 also has the same electronic structure.[17] On the clean surface of CoS_2, a spin density close to unity is found with the unpaired electron localized over the Co atom. After the S_8 adsorption, the spin densities of the Co atoms remain nearly 1. Moreover, the Bader charge of S_8 was 0.1, indicating almost no electron donation from the surface. Upon S–S bond cleavage, the spin densities of the two Co atoms strongly coordinated to terminal S atoms of the cleaved S_8 molecule decrease to 0.3, and the Bader charge of the S_8 part was −0.4, indicating that electrons are donated from the surface. These computational results suggest that the generation of S radicals is suppressed by the coupling of unpaired electrons to form bonds between the S_8 and Co atoms of the surface.

As shown in Figure S6, we performed geometry optimization starting from an initial structure that was close to an anti-Markovnikov intermediate by setting the distance to 1.8 Å between the terminal S atom of the adsorbed linear S_8 and the carbon atom of the alkene moiety of isobutene used as a model for the DFT calculations. However, no bond formation occurs, and the isobutene molecule moves away from the adsorbed S_8. Similarly, geometry optimization starting from an

initial structure with the surface S atom in close proximity to the alkene also did not result in bond formation. These computational results rule out a radical mechanism as suggested by the experimental results.

As depicted in Figure 11, we investigated the cleavage of H_2 on the CoS_2 surface. The resulting Brønsted acid sites (Co–H, S–H) are expected to be responsible for the subsequent protonation of alkenes, which gives rise to Markovnikov-type products. A H_2 molecule is adsorbed on a Co atom with an adsorption energy of –0.21 eV, which shows that the H_2 molecule can be easily desorbed. This is considered to be one of the factors requiring high pressure for the catalytic reaction. The activation energy for hydrogen molecule cleavage is 1.33 eV, relatively high in this catalytic cycle, and is 0.71 eV endothermic.

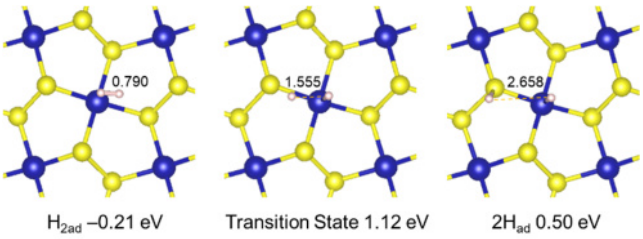

Figure 11. Adsorption and activation of the H_2 molecule on the clean (100) surfaces of CoS_2. White balls indicate H. Energies were measured from the total energy of the separated H_2 and surface. Unit is Å.

Considering the effect of co-adsorbed molecules, it was found that the cleavage of H_2 molecules adsorbed near the cleaved S_8 is promoted, as shown in Figure 12. The adsorption energy of a H_2 molecule remained unchanged at –0.21 eV, but the activation energy for the cleavage of H_2 was significantly reduced to 0.51 eV, resulting in an exothermic reaction of 0.26 eV. A second

proton transfer occurs from the resultant Co–H to HS_8. The overall reaction is endothermic with a heat of reaction of –0.14 eV.

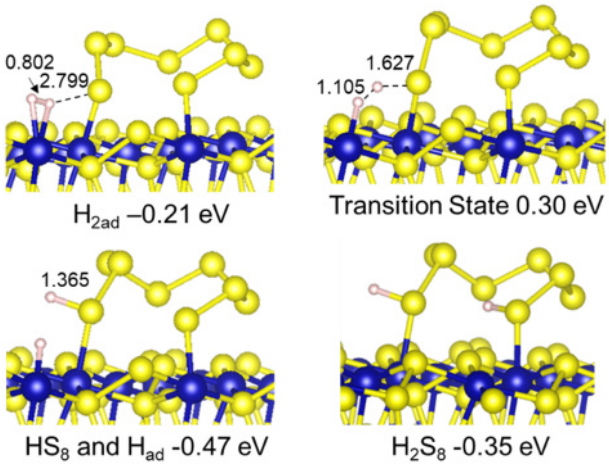

Figure 12. Adsorption and activation of the H_2 molecule on the (100) surface in the presence of the cleaved S_8. Energies were measured from the total energy of the separated H_2 and surface adsorbed with the cleaved S_8. Unit is Å.

Because Markovnikov-type thiols and polysulfanes are selectively formed in this reaction, we considered the formation of primary and tertiary carbocation intermediates by proton donation from the protonated S_8 to isobutene. As shown in Figure S7, geometry optimization was performed from an initial structure in which the primary and tertiary carbocations are hydrogen-bonded to the terminal S of S_8. However, despite increasing the hydrogen bond distance by more than 2.0 Å, the proton was transferred from the carbocations to S_8, resulting in isobutene and HS_8. This computational result rules out the formation of carbocation intermediates, which is unexpected given the high selectivity of Markovnikov-type products observed in the experiments.

Based on these computational and experimental findings, we have considered a reaction pathway, as illustrated in Figure 13, where a proton donation from HS to alkene takes place

simultaneously with the direct binding of the protonated alkene to S_8 without the formation of carbocation intermediates. In the initial stage of this pathway, an alkene molecule weakly adsorbed to the Co atom on the surface in isobutene$_{ad}$ is released to adopt a near-attack conformation (NAC), which is a required conformation for reactants to enter a transition state. This rearrangement of the alkene molecule to NAC requires an energy of 0.42 eV. In TS1_M, proton transfer from the HS moiety of HS_8 adsorbed on the surface to the alkene occurs synchronously with the formation of a bond between the other carbon of the C=C moiety of the alkene and the S atom next to the HS moiety, leading to the formation of a Markovnikov-type polysulfane intermediate, Int_M. The activation energy of this process is 0.76 eV measured from isobutene$_{ad}$ and this reaction process is almost thermoneutral. Figure S8 shows computational results for the formation of an anti-Markovnikov-type polysulfane. As expected from the experimental results, the activation energy is higher by 0.17 eV than that for the Markovnikov polysulfane. Although carbocation intermediates are not involved in this pathway, the electronic structure of the alkene moiety in the transition state is similar to that of tertiary or primary carbocations, which can be a cause of the difference in activation energy.

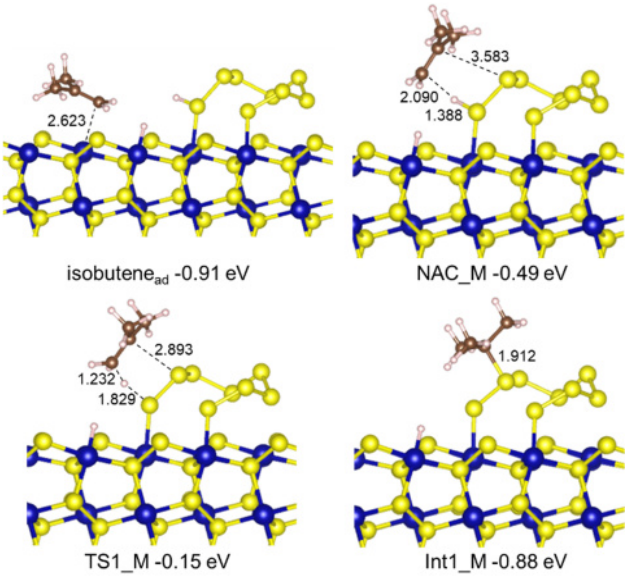

Figure 13. Optimized structures and relative energies for the formation of a Markovnikov-type polysulfane. Brown balls indicate C. Energies were measured from the total energy of the separated isobutene and surface adsorbed with HS_8 (HS_8 and Had in Figure 12). Unit is Å.

As discussed above, carbocation intermediates are not formed in this reaction pathway. This computational result is consistent with the product distribution in the time–course experiments that shows that the polysulfanes were formed in the early stages of the reaction whereas the thiols were not observed (see Table S5 in Supporting Information). These observations would be attributable to the lack of a long lifetime carbocation which can directly afford the corresponding thiol product via C–S bond formation with the surface S atom. The majority of the activation energy, 0.42 eV out of the total 0.76 eV, is required for the formation of NAC. This energy is used to take away the alkene from the surface and bring it closer to the HS and adjacent S atom of HS_8. As discussed above, the carbocation intermediate is not formed by the proton donation from HS_8. In the initial structure used for structure optimization in Figure S7(a), the central C atom of the carbocation is closest to the surface S atom (4.1 Å) rather than the S atom of S_8, but neither does the carbocation bind to the surface S atom upon structure optimization. Additionally, we investigated a reaction

pathway where the protonation from HS_8 to the alkene and the formation of the C–S bond between the alkene and the surface S atom occurs in a single step. However, we cannot obtain an appropriate initial structure for the corresponding transition state due to the presence of the surface. Thus, the formation of the long-lived carbocations is suppressed, and consequently the formation of the thiol, which is not observed as a product in the early stage of the catalysis, is also suppressed. These computational results suggest that the reaction proceeds to generate polysulfanes only when the alkene adopts a configuration close to the HS_8 as in the NAC, which provides a plausible explanation for the observed high selectivity towards Markovnikov-type polysulfanes in the experiments.

A possible reaction mechanism is proposed in Scheme 6. Initially, Co_3O_4 is subjected to sulfurization to form cobalt sulfide species (Co_xS_y). Subsequently, S–S bond cleavage of the S_8 proceeds followed by heterolytic H_2 activation with the cobalt polysulfide species.[18] The terminal SSH group in the cobalt polysulfide undergoes protonation of the alkene substrate and simultaneous Markovnikov-type C–S bond formation. Further addition to alkene, disproportionation,[19] nucleophilic S–S bond exchange with RS_nH,[9c] and/or dehydrogenative S–S bond formation would lead to the formation of dialkylpolysulfanes.[20] The polysulfane products would also undergo hydrogenolysis or exchange reaction of the S–S bonds, and the product distribution would depend on their kinetic and thermal stabilities under the reaction conditions.

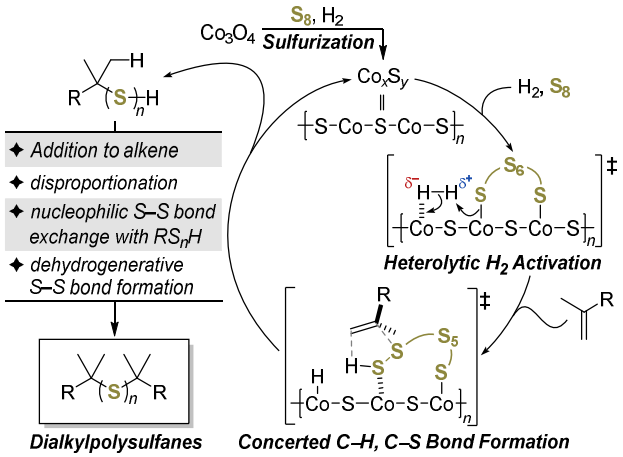

Scheme 6. Proposed reaction mechanism.

In this study, we have successfully developed a novel H_2S-reagent-free catalytic reaction for the dialkylpolysulfane synthesis using alkenes, elemental sulfur, and hydrogen. The Co_3O_4 and Na-X zeolite catalyst system efficiently promoted the reaction of DIB to provide the corresponding Markovnikov-type dialkylpolysulfanes (RS_nR: n = 2–8) in up to 88% yield, which is comparable to the current industrial process. In addition, the catalyst showed excellent durability and could be reused at least 10 times without significant loss of yield. Furthermore, the results of the characterization of the catalysts with XRD, XPS, STEM, and EDS indicate the sulfurization of Co_3O_4 to cobalt sulfides under the reaction conditions. DFT mechanistic studies suggest the heterolytic H_2 activation with the cobalt polysulfide species and subsequent concerted C–H and C–S bond formations with the SSH group. Further investigations of the substrate scope and improvement of the catalyst activity are now underway.

ASSOCIATED CONTENT

Supporting Information

The following files are available free of charge.

Experimental details and data, NMR spectra, computational details (PDF)

Data for optimized structures (VASP)

AUTHOR INFORMATION

Corresponding Author

Eiji Yamamoto − Department of Chemistry, Graduate School of Science, Kyushu University, 744 Motooka, Nishi-ku, Fukuoka, 819-0395, Japan; orcid.org/0000-0001-5968-8186; E-mail: eiyam@chem.kyushu-univ.jp

Takashi Kamachi − Department of Life, Environment and Applied Chemistry, Fukuoka Institute of Technology, 3-30-1 Wajiro-higashi, Higashi-ku, Fukuoka, 811-0295, Japan; orcid.org/0000-0001-9281-0454; E-mail: kamachi@fit.ac.jp

Makoto Tokunaga − Department of Chemistry, Graduate School of Science, Kyushu University, 744 Motooka, Nishi-ku, Fukuoka, 819-0395, Japan; orcid.org/0000-0003-1032-3199; E-mail: mtok@chem.kyushu-univ.jp

ACKNOWLEDGMENT

A part of this work was supported by "Advanced Research Infrastructure for Materials and Nanotechnology in Japan (ARIM)" of the Ministry of Education, Culture, Sports, Science and Technology (MEXT). Proposal Number JPMXP12yyxx1234. Computations were partially carried out using the computer facilities at the Research Institute for Information Technology, Kyushu University.

REFERENCES

(1)(a) Chauvin, J.-P. R.; Griesser, M.; Pratt, D. A. The antioxidant activity of polysulfides: it's radical!. *Chem. Sci.* **2019**, *10*, 4999–5010. (b) Qian, E. W.; Yamada, S.; Lee, J.; Otsuki, S.; Ishii, M.; Ota, D.; Hiirabayashi, K.; Ishihara, A.; Kabe, T. Synthesis of polysulfides using diisobutylene, sulfur, and hydrogen sulfide over solid base catalysts. *Appl*. *Catal*. *A Gen*. **2003**, *253*, 15–27. (c) Yamada, S.; Qian, W.; Ishihara, A.; Wang, G.; Li, L.; Kabe, T. Methods of Activating Catalysts for Hydrodesulfurization of Light Gas Oil (Part 1) Catalytic Activity of $CoMo/Al_2O_3$ Catalyst Presulfided with Polysulfides for Hydrodesulfurization of Dibenzothiophene. *J. Jpn. Petro. Inst.* **2001**, *44*, 217–224.

(2) Rudnick, L. R. Ed., *Lubricant Additives Chemistry and Applications*; 3rd ed.; CRC Press, Boca Raton, **2017**.

(3)(a) Farng, L. O.; Jao, T.-C. Ashless Antiwear and Antiscuffing (Extreme Pressure) Additives. In *Lubricant Additives Chemistry and Applications*, 3rd ed.; Rudnick, L. R., Eds.; CRC Press, Boca Raton, **2017**, pp. 120–121. (b) Takaki, T.; Yagishita, K.; Tsujimoto, T.; Wakabayashi, T. Influence of Organo-Sulfur Compounds with Overbased Calcium Compounds on Lubrication in Cold Forming. *Lubricants* **2017**, *5*, 8.

(4) Vineyard, B. D. The Vesatility and the Mechanism of the *n*-Butylamine-Catalyzed Reaction of Thiols with Sulfur. *J. Org. Chem.* **1967**, *32*, 3833–3836.

(5) Arisawa, M.; Tanaka, K.; Yamaguchi, M. Rhodium-catalyzed sulfur atom exchange reaction between organic polysulfides and sulfur. *Tetrahedron Lett.* **2005**, *46*, 4797–4800.

(6) Fährmann, J.; Hilt, G. Electrochemical Synthesis of Organic Polysulfides from Disulfides by Sulfur Insertion from S_8 and an Unexpected Solvent Effect on the Product Distribution. *Chem. Eur. J.* **2021**, *27*, 11141–11149.

(7) (a) Ishihara, A.; Eika, Q.; Kabe, T.; Yamada, S. Production method for alkene sulfides. JP 2004-249965, August 30, 2004. (b) Yamada, S.; Numada, H. Production method for alkene sulfides. JP H10-053372, March 5, 1998.

(8) For a review related to the organic synthesis using elemental sulfur; see: Nguyen, T. B. Recent Advances in Organic Reactions Involving Elemental Sulfur. *Adv. Synth. Catal.* **2017**, *359*, 1066–1130.

(9) For recent our reports related to heterogeneous catalysis; see: (a) Kawai, Y.; Haruguchi, K.; Sumikawa, K.; Kawada, M.; Yamamoto, E.; Murayama, H.; Tokunaga, M. Aerobic oxidation of isoprene glycol with platinum-bismuth nanoparticles catalysts supported on metal oxides. *Appl. Catal. A Gen.* **2022**, *643*, 118781. (b) Huang, Q.-A.; Ikeda, T.; Haruguchi, K.; Kawai, S.; Yamamoto, E.; Murayama, H.; Ishida, T.; Honma, T.; Tokunaga, M. Intramolecular cyclization of alkynoic acid catalyzed by Na-salt-modified Au nanoparticles supported on metal oxides. *Appl. Catal. A Gen.* **2022**, *643*, 118765. (c) Yamamoto, E.; Kawai, Y.; Takakura, K.; Kimura, M.; Murayama, H.; Matsueda, H.; Otsuki, S.; Sakata, H.; Tokunaga, M. Convenient Unsymmetrical

Disulfane Synthesis: Basic Zeolite-Catalyzed Thiol-Disulfane Exchange Reaction. *ChemCatChem* **2021**, *13*, 4694–4699. (d) Huang, Q.-A.; Haruta, A.; Kumamoto, Y.; Murayama, H.; Yamamoto, E.; Honma, T.; Okumura, M.; Nobutou, H.; Tokunaga, M. Pt/CeO_2 with residual chloride as reusable soft Lewis acid catalysts: Application to highly efficient isomerization of allylic esters. *Appl. Catal. B Environ.* **2021**, *296*, 120333.

(10) Farlow, M. W.; Lazier, W. A.; Signaig, F. K. Catalytic Synthesis of Thiols. *Ind. Eng. Chem.* **1950**, *42*, 2547–2539.

(11) Topsøe, H.; Clausen, B. S.; Massoth F. E. *Hydrotreating Catalysis, Science and Technology*; Springer-Verlag, Heidelberg, **1996**. (b) Toshiaki, K.; Atsushi, I.; Weihua, Q. *Hydrodesulfurization and Hydrodenitrogenation: Chemistry and Engineering*; Wiley-VCH, Tokyo, **1999**. (c) Sánchez-Delgado, R. A. *Organometallic Modeling of the Hydrodesulfurization and Hydrodenitrogenation Reactions*; Springer, Dordrecht, Netherlands, **2002**.

(12) Picard, J. P.; Baud, G.; Besse, J. P.; Chevalier, R. Croissance crystalline et étude structural de Co_3O_4. *J. Less-common met.* **1980**, *75*, 99–104.

(13) Lundqvist, D.; Westgren, A. Röntgenuntersuchung des Systems Co–S. Z. *Anorg. Allg. Chem.* **1938**, *239*, 85–88.

(14) (a) Aloqayli, S.; Ranaweera, C. K.; Wang, Z.; Siam, K.; Kahol, P. K.; Tripathi, P.; Srivastava, O. N.; Gupta, B. K.; Mishra, S. R.; Perez, F.; Shen, X.; Gupta, R. K. Nanostructured cobalt oxide and cobalt sulfide for flexible, high performance and durable supercapacitors. *Energy Storage Mater.* **2017**, *8*, 68–76. (b) Chen, C.-J.; Chiang, R.-K. Sulfidation of rock-salt-type transition metal oxide nanoparticles as an example of a solid state reaction in colloidal nanoparticles. *Dalton Trans.*

2011, *40*, 880–885. (c) Seo, J.-W.; Jun, Y.-W.; Park, S.-W.; Nah, H.; Moon, T.; Park, B.; Kim, J.-G.; Kim, Y. J.; Cheon, J. Two-Dimensional Nanosheet Crystals. *Angew. Chem. Int. Ed.* **2007**, *46*, 8828–8831. (d) Li, X.; Chu, H.; Li, Y. Sacrificial template growth of CdS nanotubes from $Cd(OH)_2$ nanowires. *J. Solid State Chem.* **2006**, *179*, 96–102.

(15) Li, B.; Xing, R.; Mohite, S. V.; Latthe, S. S.; Fujishima, A.; Liu, S.; Zhou, Y. CoS_2 nanodots anchored into heteroatom-doped carbon layer via a biomimetic strategy: Boosting the oxygen evolution and supercapacitor performance. *J. Power Sources* **2019**, *436*, 226862.

(16) Sheng, H.; Hermes, E. D.; Yang, X.; Ying, D.; Janes, A. N.; Li, W.; Schmidt, J. R.; Jin, S. Electrocatalytic Production of H_2O_2 by Selective Oxygen Reduction Usng Earth-Abundant Cobalt Pyrite (CoS_2). *ACS Catal.* **2019**, *9*, 8433–8442.

(17) (a) Yamada, H.; Terao, K.; Aoki, M. Electronic structure and magnetic properties of CoS_2. *J. Magn. Magn. Mater.* **1998**, 177–181, 607–608. (b) Wang, R. Z.; Zhang, Y. Magnetism modulation of Co_3S_4 towards the efficient hydrogen evolution reaction. *Mol. Syst. Des. Eng.* **2020**, *5*, 565–572.

(18) For reviews about heterolytic H_2 activation in hetergeneous catalysis; see: (a) Jing, Y.; Wang, Y. *Chem Catalysis* **2023**, *3*, 100515. (b) Aireddy, D. R.; Ding, K. Heterolytic Dissociation of H_2 in Heterogeneous Catalysis. *ACS Catal.* **2022**, *12*, 4707–4723. (c) Ma, Y.; Zhang, S.; Chang, C.-R.; Huang, Z.-Q.; Ho, J. C.; Qu, Y. Semi-solid and solid frustrated Lewis pair catalysts. *Chem. Soc. Rev.* **2018**, *47*, 5541–5553. (d) Stephan, D. W. Frustrated Lewis Pairs: From Concept to Catalysis. *Acc. Chem. Res.* **2015**, *48*, 306–316.

(19) Pickering, T. L.; Saunders, K. J.; Tobolsky, A. V. Disproportionation of Organic Polysulfides. *J. Am. Chem. Soc.* **1967**, *89*, 2364–2367.

(20) For a review about the chemistry of polysulfanes; see: Steudel, R. The Chemistry of Organic Polysulfanes R–S_n–R (n >2). *Chem. Rev.* **2002**, *102*, 3905–3945.

TOC

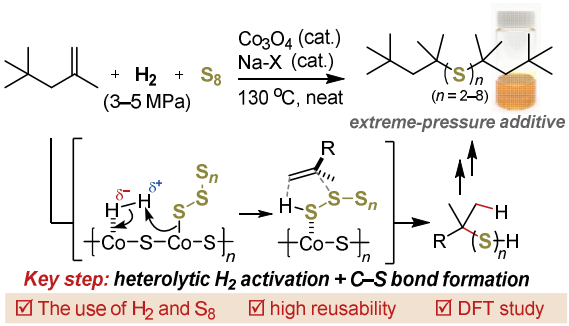
+ H2 + S8
(3–5 MPa)
Co3O4 (cat.)
Na-X (cat.)
130 °C, neat
(n = 2–8)
extreme-pressure additive
Key step: heterolytic H2 activation + C–S bond formation
☑ The use of H2 and S8
☑ high reusability
☑ DFT study